machines

MDPI

Article

Adaptive Sliding Mode Predictive Control for Path Tracking of Wheeled Agricultural Vehicles

Wenlong Liu [1,2,3], Rui Guo [1,3,*] and Jingyi Zhao [1,4]

[1] School of Mechanical Engineering, Yanshan University, Qinhuangdao 066004, China; liuwenlong@stumail.ysu.edu.cn (W.L.); zjy@ysu.edu.cn (J.Z.)
[2] Department of Electrical & Information Engineering, Qinhuangdao Campus, Northeast Petroleum University, Qinhuangdao 066004, China
[3] Hebei Key Laboratory of Special Carrier Equipment, Yanshan University, Qinhuangdao 066004, China
[4] Limited Company of Yanda-Yihua Electromechanical Engineering Technology Research Institute, Qinhuangdao 066004, China
* Correspondence: guorui@ysu.edu.cn

Abstract: This study presents an adaptive sliding mode predictive control (ASMPC) algorithm intended to improve the control precision and robustness of path tracking for wheeled agricultural vehicles. Firstly, the kinematics state equations of the vehicle were established based on path tracking errors. Secondly, in order to design the path tracking controller by combining the precision advantage of model predictive control (MPC) algorithm with the robustness advantage of sliding mode control (SMC) algorithm, the sliding mode functions were designed and used as the output equations to establish the kinematics state space model of the vehicle. Thirdly, on the basis of linearization and discretization for the kinematics state space model, the control law of path tracking was obtained using the MPC algorithm. Finally, according to the fuzzy rules designed by the working speed of the vehicle and the curvature of the reference path, the prediction horizon and control horizon of the MPC algorithm were adaptively adjusted to further improve the control precision and robustness of the path tracking system. The results of CarSim and MATLAB/Simulink co-simulation show that the proposed ASMPC algorithm is superior to the traditional SMC algorithm and conventional MPC algorithm in terms of control precision, dynamic performance, and robustness. The results of our field test show that the root mean square (RMS) values of the lateral errors for straight path tracking and curve path tracking do not exceed 2.1 and 8.7 cm, respectively, in the speed range of 1.0 to 3.5 m/s, suitable for field working. The control precision and robustness of the proposed ASMPC algorithm can meet the working requirements of wheeled agricultural vehicles.

Keywords: wheeled agricultural vehicle; path tracking; sliding mode control; model predictive control; fuzzy logic

check for updates

Academic Editor: Junyong Zhai

Received: 17 January 2025
Revised: 13 February 2025
Accepted: 14 February 2025
Published: 17 February 2025

Citation: Liu, W.; Guo, R.; Zhao, J. Adaptive Sliding Mode Predictive Control for Path Tracking of Wheeled Agricultural Vehicles. *Machines* **2025**, *13*, 157. https://doi.org/10.3390/machines13020157

Copyright: © 2025 by the authors. Licensee MDPI, Basel, Switzerland. This article is an open access article distributed under the terms and conditions of the Creative Commons Attribution (CC BY) license (https://creativecommons.org/licenses/by/4.0/).

1. Introduction

The automatic driving of agricultural vehicles via automatic navigation technology and path tracking technology is key to achieving precise agriculture and building unmanned farms [1,2]. Automatic navigation systems usually adopt an integrated navigation methodology to obtain the position, speed, attitude, and other information of the vehicle in real time, while the path tracking system changes the steering angle of the vehicle by means of a hydraumatic drive or motor drive, so that the vehicle travels along the reference path [3–6]. An automatic driving system can significantly improve the working

quality, production efficiency, and safety issues of agricultural vehicles and is widely used in agricultural production processes such as ploughing, ridging, seeding, fertilizing, and harvesting [7,8]. When the automatic navigation system precisely obtains the position and attitude of the vehicle, the working precision and dynamic performance of the automatic driving system depend on the control algorithm for path tracking [9]. Therefore, many control algorithms, such as pure pursuit control [10–12], Stanley control [13,14], PID control [15–17], and optimal control [18,19], have been successively applied to the path tracking of agricultural vehicles. The path tracking process of an agricultural vehicle is inevitably affected by uncertain factors from the unique working environment of farmland. However, the design principle of the above control algorithms determines whether it is difficult to ensure good path tracking performance for an agricultural vehicle in a complex working environment [20].

The sliding mode control (SMC) algorithm, which is an effective control algorithm for nonlinear systems, has strong robustness because of the invariance of sliding mode relative to parameter variations and external disturbance, making it suitable for the path tracking control of agricultural vehicles in complex working environments [21]. The inherent chattering phenomenon of the SMC algorithm affects the precision and dynamic performance of control systems. Therefore, chattering suppression becomes a problem that must be solved when using the SMC algorithm [20]. A high performance adaptive SMC algorithm for the path tracking of an agricultural vehicle was proposed, using a sliding mode observer to estimate the dynamic system state of the vehicle in real time and adjusting the limit value of tire cornering stiffness online [22]. A lateral error model of an agricultural tractor was established based on preview kinematics laws, and then a second-order SMC algorithm was designed with the adaptive adjustment of the control gain [23]. The second-order SMC algorithm improved the response speed and anti-disturbance ability of the tractor path tracking system. A three-order SMC algorithm was designed to realize the straight path tracking of agricultural tractors effectively [24]. A non-singular terminal SMC algorithm was proposed based on an adaptive disturbance observer, which made the path tracking errors of agricultural tractors converge to any small neighborhood near the origin in a fixed time [25]. In order to solve the fast on-line problem of straight path tracking for agricultural tractors, a fast SMC algorithm was proposed with parameter adjustments [26]. In the above-mentioned research on the SMC algorithm, many improvement measures, such as adjusting parameters dynamically, designing the disturbance observer, and improving the sliding mode order, were adopted to reduce the effects of chattering and maximize the advantages of the robustness of the SMC algorithm, but the complementary fusion of the SMC algorithm and other control algorithms were not fully considered.

The model predictive control (MPC) algorithm is a kind of advanced control algorithm based on a prediction model, rolling optimization, and feedback correction; it has high control precision and strong optimization ability for multi-objective constraint problems [27]. On the basis of the linearization and discretization of a transplanter for the kinematics model, a linear time-varying MPC controller for path tracking was designed [28]. In order to avoid the errors caused by model linearization, a nonlinear MPC algorithm for path tracking was proposed based on direct discretization of the kinematics model for an agricultural vehicle [29]. An improved particle swarm optimization algorithm was adopted to adjust the prediction horizon of the linear time-varying MPC algorithm online so as to improve the robustness of the path tracking system for agricultural tractors [30]. A linear parameter varying lateral model of an autonomous vehicle was built by considering tire nonlinear characteristics and time-varying vehicle speed, and then an MPC-based path tracking controller with strong robustness was designed through a set of linear matrix inequalities [31]. A condensed constraint matrix method was introduced into the linear

time-varying MPC algorithm to improve the efficiency of optimization solving [32]. In the above MPC algorithm research, the path tracking performance of the linear time-varying MPC algorithm was improved through many strategies, such as replacing the linear time-varying model with a nonlinear model, adjusting the control parameters with an intelligent optimization algorithm dynamically, and considering the major uncertainties in a vehicle model. However, the amount of controller calculations increased, and the real-time performance of the path tracking system was reduced.

The sliding mode predictive control (SMPC) algorithm combining the SMC algorithm with the MPC algorithm provides the complementary advantages of the two algorithms; it has been applied to self-driving vehicles but not agricultural vehicles. In existing research, the main types of SMPC algorithms are as follows:

(1) The SMC algorithm is used to design a disturbance observer to reduce uncertainties. On that basis, the MPC algorithm is used to design a path tracking controller [33].
(2) The SMC algorithm is adopted to design a path tracking controller, and then the MPC algorithm is used to optimize the sliding mode parameters [34].
(3) The SMC algorithm is used to design a sliding mode surface and a sliding mode approach law; then, the MPC algorithm is adopted to obtain a control law [35,36]. The control law can make the vehicle reach the sliding mode surface along the trajectory formed by the sliding mode approach law, thus realizing path tracking indirectly.

Among the above SMPC algorithms, the first two may be categorized as shallow combinations, and the third as deep combination. The first two SMPC algorithms use the MPC algorithm and the SMC algorithm to solve the control law of path tracking, while the third SMPC algorithm uses the MPC algorithm and the SMC algorithm to solve the control law of path tracking. As a result, the third SMPC algorithm can better integrate the control advantages of the MPC algorithm and the SMC algorithm.

This paper focuses on the path tracking of wheeled agricultural vehicles. In order to improve the precision and robustness of path tracking, a path tracking error model of a vehicle was established using kinematics methodologies, and then an adaptive sliding mode predictive control (ASMPC) algorithm was proposed to design a path tracking controller. On the basis of the third SMPC algorithm, the ASMPC algorithm was improved as follows: The sliding mode approach law was not used in order to ensure the speediness of the path tracking system, and the prediction horizon was adaptively adjusted by the fuzzy logic methodology to enhance the robustness of the path tracking system.

2. ASMPC Algorithm Design for Path Tracking

2.1. Kinematics Modeling of Wheeled Agricultural Vehicle

The actual working speed of an agricultural vehicle is low, and the lateral force on the tires is very small. Without considering the cornering characteristics of the tires, a four-wheeled agricultural vehicle can be simplified into a two-wheeled bicycle for kinematics modeling [37]. The four-wheeled agricultural vehicle generally adopts the working mode of front-wheel steering and rear-wheel drive, so the center point of the rear axle is selected to describe the position of the vehicle. The established kinematics model of the vehicle is shown in Figure 1. XOY and $X'AY'$ are the inertial coordinate system and Frenet coordinate system, respectively, where S is the reference path, A is the current target point on the path S with coordinates (x_r, y_r) in the coordinate system XOY, H is the center point of the rear axle for the vehicle with coordinates (x_c, y_c) in the coordinate system XOY and coordinates (x, y) in the coordinate system $X'AY'$, where y is also the lateral error of the vehicle, θ_r is the reference heading angle, θ_c is the heading angle of the vehicle, θ is the heading error of the vehicle, δ is the front-wheel steering angle of the vehicle, and l is the wheelbase of the vehicle.

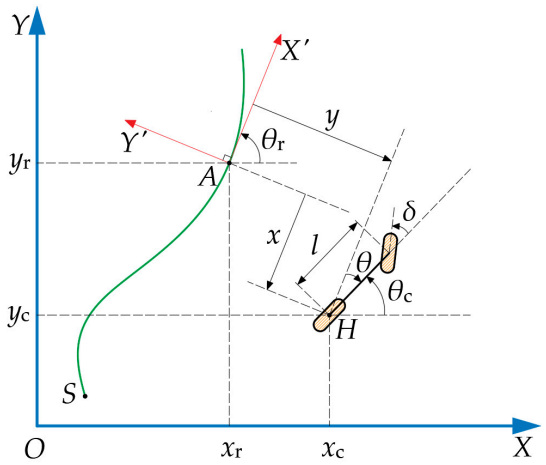


Figure 1. Kinematics model of wheeled agricultural vehicle.

In the inertial coordinate system XOY, the motion equations for the vehicle are described in [37].

$$\begin{cases} \dot{x}_c = v\cos\theta_c \\ \dot{y}_c = v\sin\theta_c \\ \dot{\theta}_c = v\tan\delta/l \end{cases} \tag{1}$$

where v is the working speed of the vehicle.

In Figure 1, the inertial coordinate system XOY is translated from origin O to point A, and then rotated counterclockwise around point A at angle θ_r to coincide with the Frenet coordinate system $X'AY'$. Therefore, by coordinate transformation, the position errors and heading error of the vehicle can be obtained as

$$\begin{bmatrix} x \\ y \\ \theta \end{bmatrix} = \begin{bmatrix} \cos\theta_r & \sin\theta_r & 0 \\ -\sin\theta_r & \cos\theta_r & 0 \\ 0 & 0 & 1 \end{bmatrix} \begin{bmatrix} x_c - x_r \\ y_c - y_r \\ \theta_c - \theta_r \end{bmatrix} \tag{2}$$

The given reference path S can be described by the motion trajectory of a reference vehicle, that is, target point A on path S at every moment satisfies Formula (1) and can be expressed as

$$\begin{cases} \dot{x}_r = v\cos\theta_r \\ \dot{y}_r = v\sin\theta_r \\ \dot{\theta}_r = v\tan\delta_r/l \end{cases} \tag{3}$$

where $\delta_r = \arctan(l\kappa_r)$ is the reference value of the front-wheel steering angle for the vehicle, and κ_r is the curvature of the reference path S at the point A.

By inserting Formulas (1) and (3) into the derivative expression of Formula (2), the state equations for the position errors and heading error of the vehicle are obtained as

$$\begin{cases} \dot{x} = yv\tan\delta_r/l + v\cos\theta - v \\ \dot{y} = -xv\tan\delta_r/l + v\sin\theta \\ \dot{\theta} = v\tan\delta/l - v\tan\delta_r/l \end{cases} \tag{4}$$

2.2. Design of Sliding Mode Functions

In order to ensure the stability of sliding mode motion, the Lyapunov methodology was used to design sliding mode functions. The Lyapunov function was selected as

$$V = \frac{1}{2}y^2 \tag{5}$$

Combining Formula (4) with Formula (5), the derivative of the Lyapunov function was calculated as

$$\dot{V} = y\dot{y} = y(-xv\tan\delta_r/l + v\sin\theta) \tag{6}$$

If two equations are given as

$$\begin{cases} x = 0 \\ \theta = -\arctan(vy) \end{cases} \tag{7}$$

Formula (6) may be transformed as

$$\dot{V} = -yv\sin[\arctan(vy)] = -yv\frac{vy}{\sqrt{1+v^2y^2}} \le 0 \tag{8}$$

According to the above conclusion, the sliding mode functions were designed as

$$\begin{cases} s_1 = x \\ s_2 = \theta + \arctan(vy) \end{cases} \tag{9}$$

As long as the sliding mode variables s_1 and s_2 are kept equal to 0 by control action, the lateral error y and the heading error θ can asymptotically converge to 0, so as to realize path tracking.

2.3. Design of MPC Controller

2.3.1. Output Prediction

Following the small angle assumption methodology in [38], Formula (4) may be approximately linearized as

$$\begin{cases} \dot{x} = yv\tan\delta_r/l \\ \dot{y} = -xv\tan\delta_r/l + v\theta \\ \dot{\theta} = vu/l \end{cases} \tag{10}$$

where u = tan δ–tan δ_r is the control variable.

Defining the linear coefficient α as

$$\alpha = \frac{\arctan(vy)}{y} \tag{11}$$

Formula (9) may be transformed as

$$\begin{cases} s_1 = x \\ s_2 = \theta + \alpha y \end{cases} \tag{12}$$

Combining Formula (10) with Formula (12), the kinematics state space model of the vehicle was obtained as

$$\begin{cases} \dot{\boldsymbol{\chi}} = \boldsymbol{A}\boldsymbol{\chi} + \boldsymbol{b}u \\ \boldsymbol{\eta} = \boldsymbol{c}\boldsymbol{\chi} \end{cases} \tag{13}$$

where $\boldsymbol{\chi} = [x\ y\ \theta]^T$ represents the state vector, $\boldsymbol{\eta} = [s_1\ s_2]^T$ represents the output vector, and the other parameters are defined as follows:

$$\boldsymbol{A} = \begin{bmatrix} 0 & v\tan\delta_r/l & 0 \\ -v\tan\delta_r/l & 0 & v \\ 0 & 0 & 0 \end{bmatrix},\ \boldsymbol{b} = \begin{bmatrix} 0 \\ 0 \\ v/l \end{bmatrix},\ \boldsymbol{c} = \begin{bmatrix} 1 & 0 & 0 \\ 0 & \alpha & 1 \end{bmatrix}$$

Formula (13) can be discretized as

$$\begin{cases} \boldsymbol{\chi}(k+1) = \boldsymbol{A}_k\boldsymbol{\chi}(k) + \boldsymbol{b}_k u(k) \\ \boldsymbol{\eta}(k) = \boldsymbol{c}_k\boldsymbol{\chi}(k) \end{cases} \tag{14}$$

where $\boldsymbol{A}_k$= $T\boldsymbol{A}$ + $\boldsymbol{I}$, $\boldsymbol{b}_k$= $T\boldsymbol{b}$, $\boldsymbol{c}_k$ = $\boldsymbol{c}$, $\boldsymbol{I}$ represents the unit matrix, and T represents the sampling period.

Considering the implementation of the MPC algorithm and the processing of input constraints, the control increment Δu was usually selected as the input variable, and then Formula (14) was transformed as

$$\begin{cases} \boldsymbol{\xi}(k+1) = \widetilde{\mathbf{A}}_k\boldsymbol{\xi}(k) + \widetilde{\mathbf{b}}_k\Delta u(k) \\ \boldsymbol{\eta}(k) = \widetilde{\mathbf{c}}_k\boldsymbol{\xi}(k) \end{cases} \tag{15}$$

where $\boldsymbol{\xi}(k) = [\boldsymbol{\chi}(k)\ u(k\text{-}1)]^{\mathrm{T}}$ represents the new state vector, $\Delta u(k) = u(k) - u(k\text{-}1)$, and the other parameters are defined as follows:

$$\widetilde{\boldsymbol{A}}_k = \begin{bmatrix} \boldsymbol{A}_k & \boldsymbol{b}_k \\ 0 & 1 \end{bmatrix},\ \widetilde{\boldsymbol{b}}_k = \begin{bmatrix} \boldsymbol{b}_k \\ 1 \end{bmatrix},\ \widetilde{\boldsymbol{c}}_k = \begin{bmatrix} \boldsymbol{c}_k & 0 \end{bmatrix}$$

N_{p} and N_{c} represent the prediction horizon and control horizon, respectively, and $N_{\mathrm{c}} \le N_{\mathrm{p}}$. Following the methodology in [38], the values of the system output variables could be predicted by Formula (15) within the time range of $[k + 1, k + N_{\mathrm{p}}]$, the values of the system control increment could be obtained within the time range of $[k, k + N_{\mathrm{c}}-1]$, and the predictive values of the system output variables could be expressed as

$$\boldsymbol{Y}(k) = \boldsymbol{\Psi}_k\boldsymbol{\xi}(k) + \boldsymbol{\Theta}_k\Delta\boldsymbol{U}(k) \tag{16}$$

where

$$\boldsymbol{Y}(k) = \begin{bmatrix} \boldsymbol{\eta}(k+1|k) \\ \boldsymbol{\eta}(k+2|k) \\ \vdots \\ \boldsymbol{\eta}(k+N_{\mathrm{c}}|k) \\ \vdots \\ \boldsymbol{\eta}(k+N_{\mathrm{p}}|k) \end{bmatrix},\ \Delta\boldsymbol{U}(k) = \begin{bmatrix} \Delta u(k|k) \\ \Delta u(k+1|k) \\ \vdots \\ \Delta u(k+N_{\mathrm{c}}-1|k) \end{bmatrix},\ \boldsymbol{\Psi}_k = \begin{bmatrix} \widetilde{\boldsymbol{c}}_k\widetilde{\boldsymbol{A}}_k \\ \widetilde{\boldsymbol{c}}_k\widetilde{\boldsymbol{A}}_k^2 \\ \vdots \\ \widetilde{\boldsymbol{c}}_k\widetilde{\boldsymbol{A}}_k^{N_{\mathrm{c}}} \\ \vdots \\ \widetilde{\boldsymbol{c}}_k\widetilde{\boldsymbol{A}}_k^{N_{\mathrm{p}}} \end{bmatrix},\ \boldsymbol{\Theta}_k = \begin{bmatrix} \widetilde{\boldsymbol{c}}_k\widetilde{\boldsymbol{b}}_k & 0 & \cdots & 0 \\ \widetilde{\boldsymbol{c}}_k\widetilde{\boldsymbol{A}}_k\widetilde{\boldsymbol{b}}_k & \widetilde{\boldsymbol{c}}_k\widetilde{\boldsymbol{b}}_k & \cdots & 0 \\ \vdots & \vdots & \ddots & \vdots \\ \widetilde{\boldsymbol{c}}_k\widetilde{\boldsymbol{A}}_k^{N_{\mathrm{c}}}\widetilde{\boldsymbol{b}}_k & \widetilde{\boldsymbol{c}}_k\widetilde{\boldsymbol{A}}_k^{N_{\mathrm{c}}-1}\widetilde{\boldsymbol{b}}_k & \cdots & \widetilde{\boldsymbol{c}}_k\widetilde{\boldsymbol{A}}_k\widetilde{\boldsymbol{b}}_k \\ \vdots & \vdots & \ddots & \vdots \\ \widetilde{\boldsymbol{c}}_k\widetilde{\boldsymbol{A}}_k^{N_{\mathrm{p}}-1}\widetilde{\boldsymbol{b}}_k & \widetilde{\boldsymbol{c}}_k\widetilde{\boldsymbol{A}}_k^{N_{\mathrm{p}}-2}\widetilde{\boldsymbol{b}}_k & \cdots & \widetilde{\boldsymbol{c}}_k\widetilde{\boldsymbol{A}}_k^{N_{\mathrm{p}}-N_{\mathrm{c}}}\widetilde{\boldsymbol{b}}_k \end{bmatrix}$$

2.3.2. Optimization Solving

In order to ensure that the vehicle could effectively track the reference path and avoid acute changes in the control variable, the performance index function was determined as

$$J(k) = \sum_{i=1}^{N_{\mathrm{p}}} \|\boldsymbol{\eta}(k+i|k)\|_{\boldsymbol{Q}}^2 + \sum_{j=0}^{N_{\mathrm{c}}-1} \|\Delta u(k+j|k)\|_R^2 + \rho\varepsilon^2 \tag{17}$$

where $\boldsymbol{Q}$ is the output weighting matrix, R is the control weighting coefficient, ε is the relaxation factor, and ρ is the relaxation weighting coefficient. On the right side of the equal sign for Formula (17), the first term reflects the control ability of the path tracking system, the second term reflects the constraint ability of the path tracking system to the change of the control variable, and the third term is a relaxation term which is used to avoid the absence of a feasible solution in the optimization solving process of the performance index function under constraints.

Formula (17) can be expressed in vector forms as

$$J(k) = \|\boldsymbol{Y}(k)\|^2_{\boldsymbol{Q}'} + \|\Delta\boldsymbol{U}(k)\|^2_{\boldsymbol{R}'} + \rho\varepsilon^2 \tag{18}$$

where $\boldsymbol{Q}' = \boldsymbol{I}_{N_p} \otimes \boldsymbol{Q}$, $\boldsymbol{R}' = \boldsymbol{I}_{N_c} \otimes R$, $\otimes$ represents the Kronecker product.

Substituting Formula (16) into Formula (18), the performance index function may be described as

$$J(k) = \Delta\boldsymbol{u}^{\mathrm{T}}(k)\left[\boldsymbol{\Theta}_k^{\mathrm{T}}\boldsymbol{Q}'\boldsymbol{\Theta}_k + \boldsymbol{R}'\right]\Delta\boldsymbol{u}(k) + 2\boldsymbol{\xi}^{\mathrm{T}}(k)\boldsymbol{\Psi}_k^{\mathrm{T}}\boldsymbol{Q}'\boldsymbol{\Theta}_k\Delta\boldsymbol{u}(k) + \boldsymbol{\xi}^{\mathrm{T}}(k)\boldsymbol{\Psi}_k^{\mathrm{T}}\boldsymbol{Q}'\boldsymbol{\Psi}_k\boldsymbol{\xi}(k) + \rho\varepsilon^2 \tag{19}$$

where $\boldsymbol{\xi}^{\mathrm{T}}(k)\boldsymbol{\Psi}_k^{\mathrm{T}}\boldsymbol{Q}'\boldsymbol{\Psi}_k\boldsymbol{\xi}(k)$ is a constant term, which can be ignored in the optimization solving process.

Considering the steering ability of the vehicle and the safety of automatic driving, the constraints on the control variable and control increment were set as follows:

$$\begin{cases} u_{\min} \le u(k+j|k) \le u_{\max} \\ \Delta u_{\min} \le \Delta u(k+j|k) \le \Delta u_{\max} \\ j = 0, 1, 2, \cdots, N_{\mathrm{c}} - 1 \end{cases} \tag{20}$$

where $u_{\min}$ and $u_{\max}$ are the minimum and maximum of the control variable, respectively, and $\Delta u_{\min}$ and $\Delta u_{\max}$ are the minimum and maximum of the control increment, respectively.

The relationship between the control variable and the control increment is as follows:

$$\begin{cases} u(k+j|k) = u(k+j-1|k) + \Delta u(k+j|k) \\ u(k-1|k) = u(k-1) \\ j = 0, 1, 2, \cdots, N_{\mathrm{c}} - 1 \end{cases} \tag{21}$$

Combining Formula (20) with Formula (21), the constraint conditions could be expressed in matrix forms as

$$\begin{cases} \boldsymbol{U}_{\min} \le \boldsymbol{\Omega}\Delta\boldsymbol{U}(k) + \boldsymbol{U}(k-1 \le)\boldsymbol{U}_{\max} \\ \Delta\boldsymbol{U}_{\min} \le \Delta\boldsymbol{U}(k) \le \Delta\boldsymbol{U}_{\max} \end{cases} \tag{22}$$

where

$$\boldsymbol{U}_{\min} = \begin{bmatrix} u_{\min} & u_{\min} & \cdots & u_{\min} \end{bmatrix}^{\mathrm{T}}_{1\times N_{\mathrm{c}}},\ \boldsymbol{U}_{\max} = \begin{bmatrix} u_{\max} & u_{\max} & \cdots & u_{\max} \end{bmatrix}^{\mathrm{T}}_{1\times N_{\mathrm{c}}}$$

$$\Delta\boldsymbol{u}_{\min} = \begin{bmatrix} \Delta u_{\min} & \Delta u_{\min} & \cdots & \Delta u_{\min} \end{bmatrix}^{\mathrm{T}}_{1\times N_{\mathrm{c}}},\ \Delta\boldsymbol{u}_{\max} = \begin{bmatrix} \Delta u_{\max} & \Delta u_{\max} & \cdots & \Delta u_{\max} \end{bmatrix}^{\mathrm{T}}_{1\times N_{\mathrm{c}}}$$

$$\boldsymbol{U}(k-1) = \begin{bmatrix} u(k-1) & u(k-1) & \cdots & u(k-1) \end{bmatrix}^{\mathrm{T}}_{1\times N_{\mathrm{c}}},\ \boldsymbol{\Omega} = \begin{bmatrix} 1 & 0 & \cdots & \cdots & 0 \\ 1 & 1 & 0 & \cdots & 0 \\ 1 & 1 & 1 & \ddots & 0 \\ \vdots & \vdots & \ddots & \ddots & 0 \\ 1 & 1 & \cdots & 1 & 1 \end{bmatrix}_{N_{\mathrm{c}}\times N_{\mathrm{c}}}$$

The performance index function Formula (19) and the constraint conditions Formula (22) were combined, and then the optimization solving problem of the MPC algorithm was

transformed into a standard quadratic optimization problem by matrix transformations, which can be described as

$$\begin{gathered}\min_{\Delta \boldsymbol{U}(k),\varepsilon} J(k) = \frac{1}{2}\begin{bmatrix}\Delta \boldsymbol{U}^{\mathrm{T}}(k) & \varepsilon\end{bmatrix}\boldsymbol{H}_k\begin{bmatrix}\Delta \boldsymbol{U}(k)\\ \varepsilon\end{bmatrix} + \boldsymbol{g}_k^{\mathrm{T}}\begin{bmatrix}\Delta \boldsymbol{U}(k)\\ \varepsilon\end{bmatrix}, \\ \text{s.t.}\boldsymbol{\Omega}_k\begin{bmatrix}\Delta \boldsymbol{U}(k)\\ \varepsilon\end{bmatrix} \le \boldsymbol{\omega}_k\end{gathered} \tag{23}$$

where

$$\boldsymbol{H}_k = \begin{bmatrix}\boldsymbol{\Theta}_k^{\mathrm{T}}\boldsymbol{Q}'\boldsymbol{\Theta}_k + \boldsymbol{R}' & 0\\ 0 & \rho\end{bmatrix},\ \boldsymbol{g}_k = \begin{bmatrix}\boldsymbol{\xi}^{\mathrm{T}}(k)\boldsymbol{\Psi}_k^{\mathrm{T}}\boldsymbol{Q}'\boldsymbol{\Theta}_k\\ 0\end{bmatrix}$$

$$\boldsymbol{\Omega}_k = \begin{bmatrix}-1 & 0\\ 1 & 0\\ -\boldsymbol{\Omega} & 0\\ \boldsymbol{\Omega} & 0\end{bmatrix},\ \boldsymbol{\omega}_k = \begin{bmatrix}-\Delta \boldsymbol{U}_{\min}\\ \Delta \boldsymbol{U}_{\max}\\ -\boldsymbol{U}_{\min} + \boldsymbol{U}(k-1)\\ \boldsymbol{U}_{\max} - \boldsymbol{U}(k-1)\end{bmatrix}$$

The optimal sequences of the control increment $\Delta \boldsymbol{U}^*(k)$ could be obtained by solving Formula (23), and then the control variable $u(k)$ and the required front-wheel steering angle $\delta(k)$ were calculated using the first element $\Delta u^*(k\,|\,k)$ in $\Delta \boldsymbol{U}^*(k)$ as follows:

$$u(k) = u(k-1) + \Delta u^*(k|k) \tag{24}$$

$$\delta(k) = \arctan\{u(k) + \tan[\delta_{\mathrm{r}}(k)]\} \tag{25}$$

Finally, $\delta(k)$ was applied to the steering system of the vehicle. By repeating the above process in each control period, the vehicle could be controlled to realize path tracking.

2.3.3. Parameter Adjustments

According to the body parameters, working speed range, and controller hardware configuration of wheeled agricultural vehicles, the adjustment scheme of the control parameters was determined, as shown in Table 1.

Table 1. Parameter settings of the ASMPC algorithm.

Parameters	Values
Prediction horizon N_{p}	See this Section 2.3.3
Control horizon N_{c}	See this Section 2.3.3
Output weighting matrix $\boldsymbol{Q}$	$\begin{bmatrix}1 & 0\\ 0 & 1\end{bmatrix}$
Control weighting coefficient $\boldsymbol{R}$	0.3
Control variable minimum $u_{\min}$	−0.53
Control variable maximum $u_{\max}$	0.53
Control increment minimum $\Delta u_{\min}$	−0.14
Control increment maximum $\Delta u_{\max}$	0.14
Relaxation factor ε	10
Relaxation weighting coefficient ρ	1000
Sampling period T (s)	0.05

When all the MPC's parameters had been determined, the performance of the MPC controller did not meet the various motion conditions of the vehicle satisfactorily. In order to improve the robustness of the MPC controller to the changes of the working speed and the reference path curvature, prediction horizon N_{p} and control horizon N_{c} were determined as adaptive adjustment parameters [38]. The fuzzy logic methodology has the

advantages of simple design, strong adaptivity, and easy maintenance [39]. Therefore, the fuzzy logic methodology was used to optimize the prediction horizon N_p online based on working speed v and relative curvature κ_{rel} of the reference path, and then the control horizon N_c was appropriately adjusted according to prediction horizon N_p.

The relative curvature κ_{rel} was defined as

$$\kappa_{rel} = \frac{\kappa_r}{\kappa_{max}} \tag{26}$$

where κ_{max} is the curvature corresponding to the minimum turning radius of the vehicle.

Considering the working requirements and automatic driving safety, the basic domain of working speed v was set as [0 m/s, 5 m/s]. The basic domain of the relative curvature κ_{rel} was set as [0, 1]. Considering the real-time performance of the path tracking system, the basic domain of the prediction horizon N_p was set as [5, 25]. The working speed v, the relative curvature κ_{rel}, and the prediction horizon N_p were divided into five fuzzy sets: very-small (VS), small (S), medium (M), large (L), and very-large (VL). The membership functions for the fuzzy sets VS and VL were selected as Gauss functions to make the path tracking system more stable, and the membership functions for the other fuzzy sets were selected as Triangle functions to ensure the precision and speediness of the path tracking system, as shown in Figure 2.

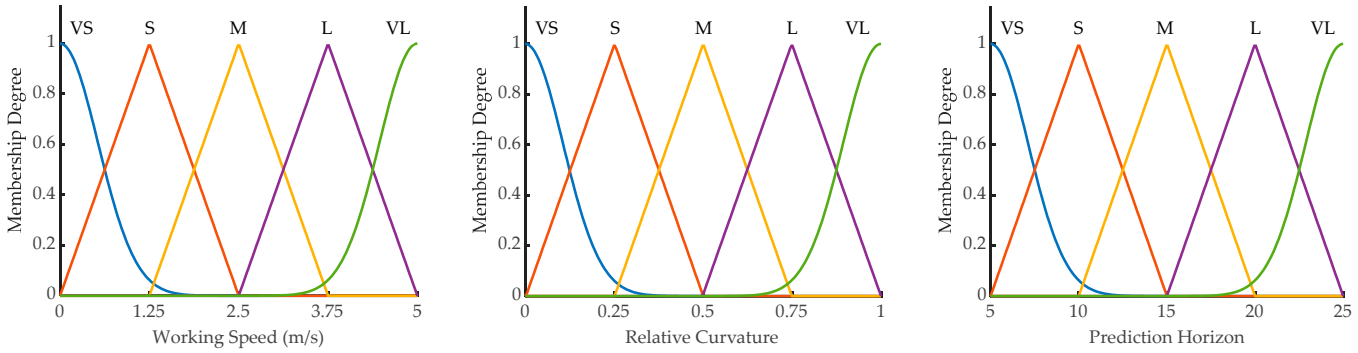


Figure 2. Membership functions. (**a**) Working speed; (**b**) Relative curvature; (**c**) Prediction horizon.

The Mamdani type of fuzzy reasoning was selected, and the design principles of fuzzy rules were as follows: When the working speed of the vehicle was high or the relative curvature of the reference path was small, the prediction horizon had to be increased to avoid the large overshoot and improve the stability of the path tracking system. Conversely, the prediction horizon had to be reduced to improve the response speed and control precision of the path tracking system. The fuzzy were are obtained by experience and simulations, as shown in Table 2 [40].

Table 2. Fuzzy rules for prediction horizon [40].

Relative Curvature	**Working Speed**				
	VS	**S**	**M**	**L**	**VL**
VS	M	L	L	VL	VL
S	S	M	L	L	VL
M	S	S	M	L	L
L	VS	S	S	M	L
VL	VS	VS	S	S	M

The fuzzy reasoning results were defuzzified with the gravity method [39]. The prediction horizon N_p was obtained by rounding operation for defuzzification results. Considering that the control horizon could be appropriately increased to improve the control precision of the path tracking system when the relative curvature of the reference path was large, the control horizon N_c could be adjusted according to the prediction horizon N_p and the relative curvature κ_{rel}, determined as

$$N_c = \text{round}\left[\beta N_p(1 + \gamma\kappa_{rel})\right] \tag{27}$$

where β is the horizon weight coefficient, $0 < \beta \leq 0.5$, γ is the curvature gain coefficient, $0 \leq \gamma \leq 1$, and round $(\cdot)$ represents the rounding operation. In this paper, β and γ are equal to 0.2 and 0.8, respectively.

3. Simulation and Result Analysis

3.1. Simulation System and Parameters

In order to verify the effectiveness of the proposed ASMPC algorithm, a John Deere 820 tractor with the parameters shown in Table 3 was used as the controlled vehicle, and then a path tracking simulation system of the vehicle was built by CarSim 2016.1 and MATLAB/Simulink R2018a, as shown in Figure 3.

Table 3. Parameters for John Deere 820 tractor.

Parameters	Values
Total mass (kg)	3190
Wheelbase l (m)	2.15
Front wheel tread (m)	1.505
Rear wheel tread (m)	1.635
Cornering stiffness of front tire (kN/rad)	73
Cornering stiffness of rear tire (kN/rad)	152
Yawing moment of inertia (kg·m^2)	11903

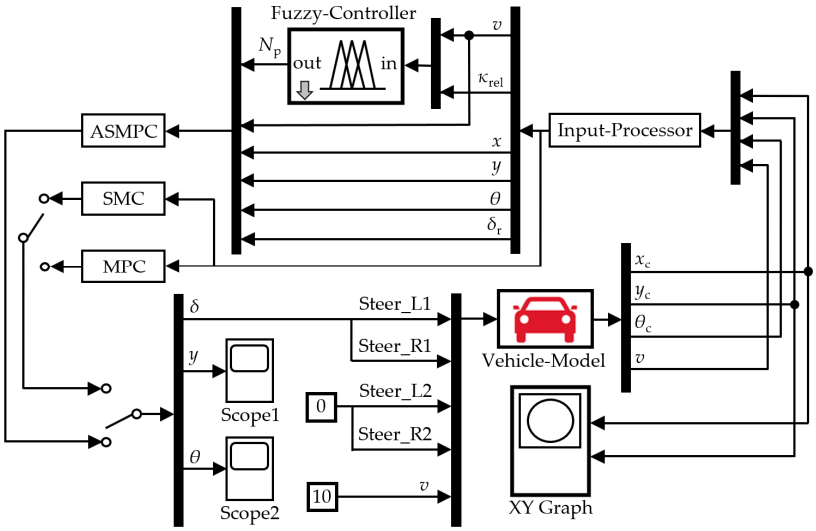


Figure 3. Simulation system of path tracking.

Assuming that the initial position and heading angle of the vehicle are (X = 0 m, Y = 0 m) and 0°, respectively, the path tracking effects of three algorithms were compared. The above algorithms include the ASMPC algorithm, the conventional MPC algorithm based on the linear time-varying model [28], and the traditional SMC algorithm based on

the exponential approach law [41]. For straight path tracking, the reference path was set as Y = 0.5 m, and the experiments were carried out at working speeds of 1, 3, and 5 m/s. For curve path tracking, the experiments were carried out at a working speed of 3 m/s, and the reference path consisted of three semicircles, including, in turn, a semicircle of center (X = 0 m, Y = 20 m) and radius 20 m, a semicircle of center (X = 0 m, Y = 25 m) and radius 15 m, and a semicircle of center (X = 0 m, Y = 20 m) and radius 10 m. The reference path was a flat concrete road with a friction coefficient of 0.75.

The parameter settings of the ASMPC algorithm are shown in Table 1. Based on practical experience and simulation research, the parameters of the conventional MPC algorithm were determined, as shown in Table 4, and the exponential approach law of the traditional SMC algorithm was determined as follows:

$$\begin{cases} \dot{s}_1 = -0.4\text{sign}(s_1) - 3s_1 \\ \dot{s}_2 = -0.5\text{sign}(s_2) - 4s_2 \end{cases} \tag{28}$$

Table 4. Parameter settings of the conventional MPC algorithm.

Parameters	Values
Prediction horizon N_p	60
Control horizon N_c	30
Output weighting matrix $\boldsymbol{Q}$	$\begin{bmatrix} 1 & 0 & 0 \\ 0 & 1 & 0 \\ 0 & 0 & 1 \end{bmatrix}$
Control weighting matrix $\boldsymbol{R}$	$\begin{bmatrix} 5 & 0 \\ 0 & 5 \end{bmatrix}$
Control variable minimum u_{min}	−0.53
Control variable maximum u_{max}	0.53
Control increment minimum Δu_{min}	−0.14
Control increment maximum Δu_{max}	0.14
Relaxation factor ε	10
Relaxation weighting coefficient ρ	1000
Sampling period T (s)	0.05

The on-line time, which is the time from the initial working state with a lateral error of 50 cm to the stable working state for a vehicle, was used to evaluate the speediness of the path tracking system. The stable working state means that the absolute value of the lateral error did not exceed 5 cm at any time, when the vehicle continued to move a distance of 5 m along the reference path direction.

The maximum absolute value and root mean square (RMS) value of the lateral error were used to evaluate the control precision of the path tracking system. When the maximum absolute value and RMS value of the lateral error were both small, it indicated that the path tracking precision was high. In addition, the approach degree between the maximum absolute value of the lateral error and the RMS value of the lateral error indirectly reflected the stability of the path tracking system. The robustness of the path tracking system could be measured according to the variation degree for the maximum absolute value and RMS value of the lateral error at different working speeds or path curvatures.

3.2. Simulation Results

The simulation results of straight path tracking for the ASMPC algorithm, the conventional MPC algorithm, and the traditional SMC algorithm are shown in Figures 4–6, respectively. The statistical data of the simulation results for the straight path tracking are shown in Table 5.

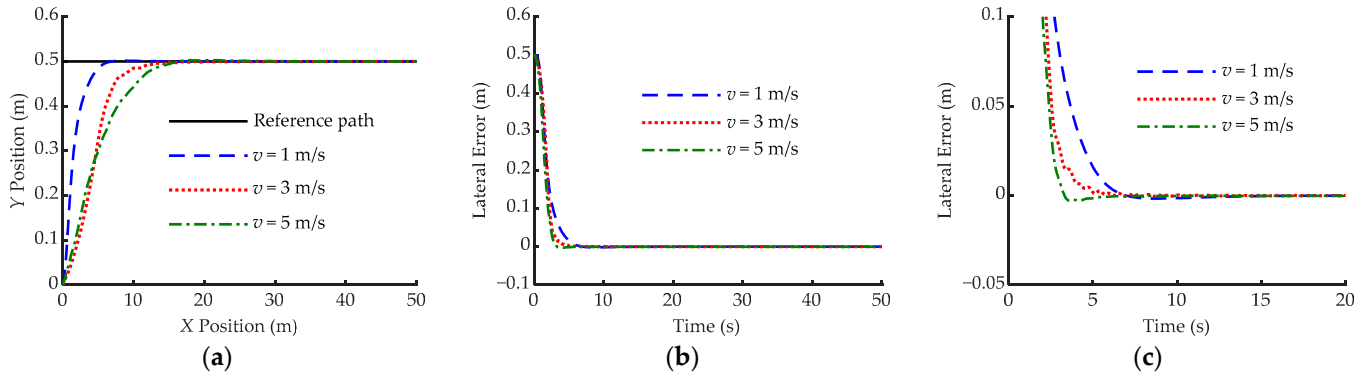


Figure 4. Simulation results of straight path tracking for ASMPC algorithm. (**a**) Tracking trajectory; (**b**) Tracking error; (**c**) Partial enlarger of tracking error.

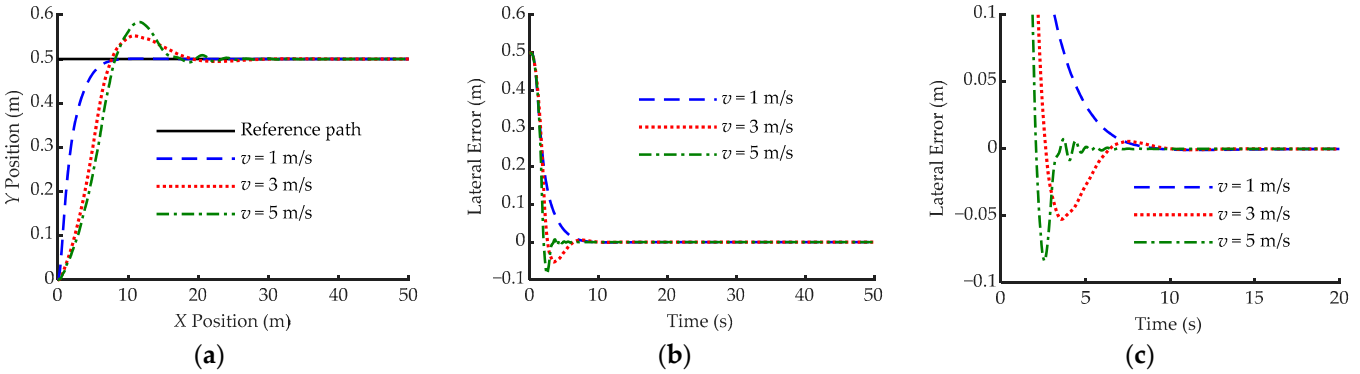


Figure 5. Simulation results of straight path tracking for conventional MPC algorithm. (**a**) Tracking trajectory; (**b**) Tracking error; (**c**) Partial enlarger of tracking error.

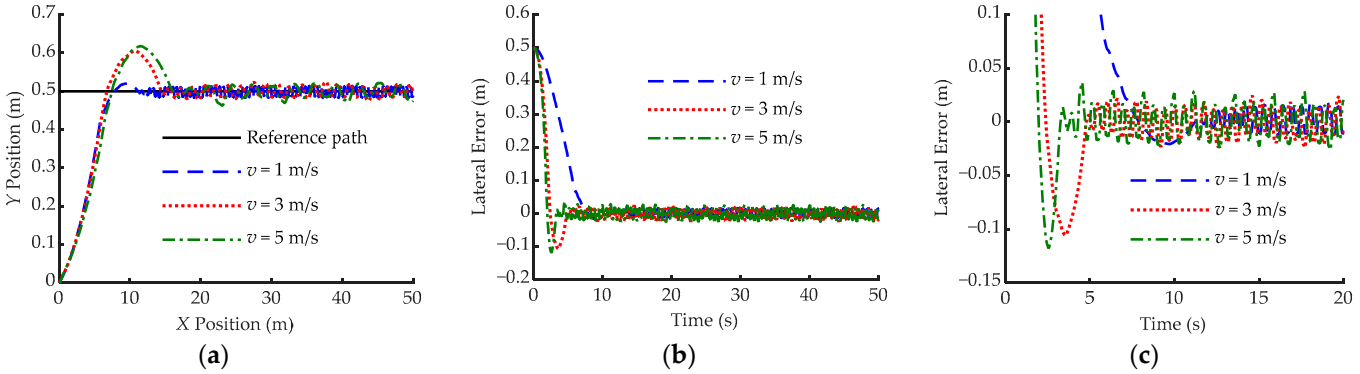


Figure 6. Simulation results of straight path tracking for traditional SMC algorithm. (**a**) Tracking trajectory; (**b**) Tracking error; (**c**) Partial enlarger of tracking error.

Table 5. Statistical data of simulation results for straight path tracking.

Algorithm	Overshoot (%)			On-Line Time (s)		
	v = 1 m/s	v = 3 m/s	v = 5 m/s	v = 1 m/s	v = 3 m/s	v = 5 m/s
ASMPC	0.34	0.09	0.60	3.7	2.6	2.4
Conventional MPC	0.16	10.52	16.70	4.4	3.9	2.9
Traditional SMC	4.12	21.16	23.56	6.5	4.5	3.1

In Figure 4, when the working speeds of straight path tracking were 1, 3, and 5 m/s, the overshoot of the ASMPC algorithm was 0.34%, 0.09%, and 0.60%, respectively, the

on-line time of the ASMPC algorithm was 3.7, 2.6, and 2.4 s, respectively, and all the lateral errors of the ASMPC algorithm asymptotically approached 0 cm. In Figure 5, when the working speeds of straight path tracking were 1, 3, and 5 m/s, the overshoot of the conventional MPC algorithm was 0.16%, 10.52% and 16.70%, respectively, the on-line time of the conventional MPC algorithm was 4.4, 3.9 and 2.9 s, respectively, and all the lateral errors of the conventional MPC algorithm asymptotically approached 0 cm. In Figure 6, when the working speeds of straight path tracking were 1, 3, and 5 m/s, the overshoot of the traditional SMC algorithm was 4.12%, 21.16% and 23.56%, respectively, and the on-line time of the traditional SMC algorithm was 6.5, 4.5, and 3.1 s, respectively. Figure 6 shows that the traditional SMC algorithm could track a straight path stably, but there was the chattering phenomenon. The magnitude of the chattering increased with the increase of the working speed. Among the above algorithms, the ASMPC algorithm had the smallest overshoot and the shortest on-line time, which indicated that the ASMPC algorithm had the best dynamic control performance. The control precision of the ASMPC algorithm without the chattering phenomenon was higher than that of the traditional SMC algorithm. Compared with the conventional MPC algorithm and the traditional SMC algorithm, the ASMPC algorithm had smaller changes of overshoot and on-line time at different working speeds, which indicated that the ASMPC algorithm had greater robustness the changes of working speed in terms of dynamic control performance.

The simulation results of curve path tracking for the ASMPC algorithm and the conventional MPC algorithm are shown in Figure 7. The statistical data of the simulation results for the curve path tracking are shown in Table 6.

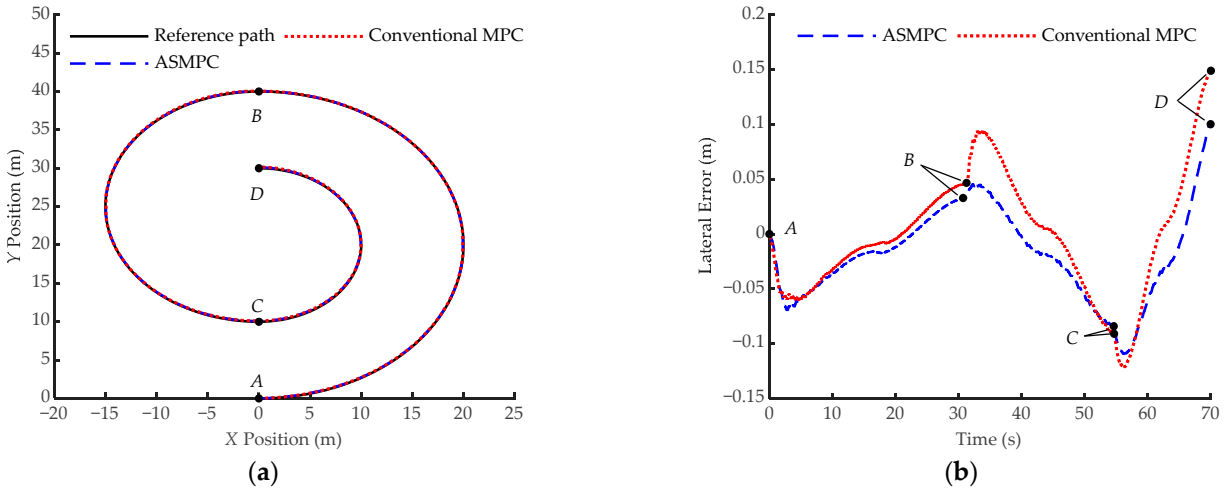


Figure 7. Simulation results of curve path tracking for ASMPC algorithm and conventional MPC algorithm at a working speed of 3 m/s. (**a**) Tracking trajectory; (**b**) Tracking error.

Table 6. Statistical data of simulation results for curve path tracking.

Algorithm	Maximum Absolute Value of Lateral Error (cm)			RMS Value of Lateral Error (cm)			
	Path *AB*	Path *BC*	Path *CD*	Path *AB*	Path *BC*	Path *CD*	Path *AD*
ASMPC	6.9	8.4	10.9	2.8	3.9	6.1	4.2
Conventional MPC	6.1	9.5	14.9	3.2	5.6	8.4	5.6

In Figure 7, both the ASMPC algorithm and the conventional MPC algorithm control the vehicle to track a curve path stably at a working speed of 3 m/s. For path segment *AB* with radius 20 m, path segment *BC* with radius 15 m, and path segment *CD* with radius 10 m, the maximum absolute values of the lateral error for the ASMPC algorithm were 6.9,

8.4, and 10.9 cm, respectively, the RMS values of the lateral error for the ASMPC algorithm were 2.8, 3.9, and 6.1 cm, respectively, the maximum absolute values of the lateral error for the conventional MPC algorithm were 6.1, 9.5, and 14.9 cm, respectively, and the RMS values of the lateral error for the conventional MPC algorithm were 3.2, 5.6, and 8.4 cm, respectively. For the whole path *AD*, the RMS values of the lateral error for the ASMPC algorithm and the conventional MPC algorithm were 4.2 and 5.6 cm, respectively. The maximum absolute values and RMS values of the lateral error for the ASMPC algorithm were smaller than those for the conventional MPC algorithm; in other words, the control precision of the ASMPC algorithm was higher than that of the conventional MPC algorithm. In addition, compared with the conventional MPC algorithm, the ASMPC algorithm had smaller changes in terms of the maximum absolute value and RMS value of the lateral error for different path curvatures, that is, the ASMPC algorithm had stronger robustness for the changes of the reference path curvature in the aspect of control precision.

4. Field Test and Result Analysis

In order to further verify the path tracking performance of the proposed ASMPC algorithm, the John Deere 820 tractor was again applied as the controlled vehicle, the global navigation satellite system (GNSS) and the inertial measurement unit (IMU) were used for the position and attitude measurement of the vehicle, and a control system for the automatic driving of the vehicle was constructed, as shown in Figure 8.

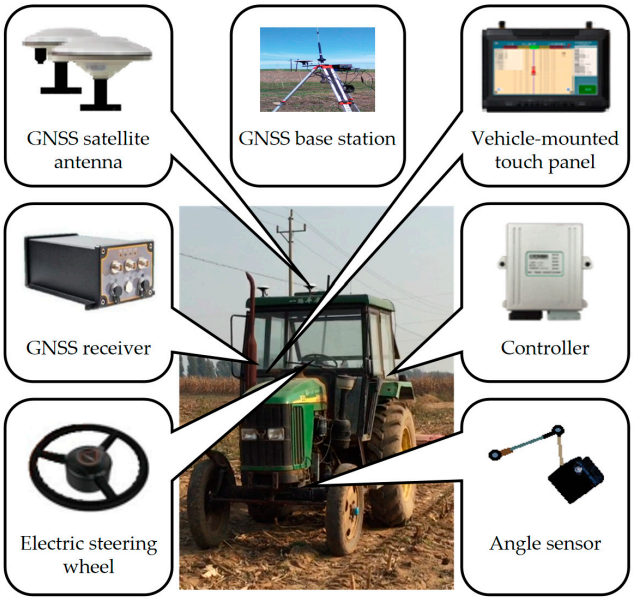


Figure 8. Control system for automatic driving.

As shown in Figure 8, the GNSS satellite antenna, GNSS receiver, angle sensor, electric steering wheel, controller, and vehicle-mounted touch panel were installed on the vehicle, and a GNSS base station was set up on the ground. The GNSS satellite antenna adopted the AT360 antenna from Shanghai Sinan Navigation Technology Inc., China, and the GNSS receiver with the positioning function of dual antenna and real-time kinematic (RTK) used the M600 receiver from Shanghai Sinan Navigation Technology Inc., China. In the RTK differential state, the positioning accuracy and heading accuracy of the M600 receiver were ± 1 cm and $\pm 0.2^{\circ}$, respectively. The angle sensor wasthe 9902120CWHT sensor from BEI Sensors, Thousand Oaks, CA, USA, which has a 12-bit A/D converter and a measurement range of -60° to 60°. The type of electric steering wheel employed was the CES-T from Shanghai Huace Navigation Technology Inc., China. The vehicle-mounted touch panel used

the JWS101-AM100 touch panel from Shenzhen Jiaweishi Electronic Science and Technology Co., Ltd., China. The controller, which had an IMU with the attitude measurement accuracy of 0.01°, was a self-developed controller using the STM32F103ZET6 microcontroller.

The tests were carried out in a dry field in Yanghetao Village, Beidaihe District, Qinhuangdao City, China. The field, with soft soil, was relatively flat, i.e., the land surface drop is less than 3 cm. Firstly, the vehicle was manually driven to the selected position *A* at the edge of the field so that the longitudinal direction of the vehicle body was consistent with the working direction. Secondly, the longitude, latitude, speed, and attitude angle of the vehicle at point *A* were obtained through the GNSS and IMU, and then the coordinates of point *A* in the Gauss plane coordinate system were calculated according to the Gauss-Kruger projection principle. Finally, the Gauss plane coordinate system was translated to point *A* and rotated by the heading angle at point *A*, thereby obtaining the inertial coordinate system *XOY*.

In the inertial coordinate system *XOY*, a reference path consisting of three straight lines and two semicircles was set, and the vehicle with the initial heading angle of 0° started from point *A* (*X* = 0 m, *Y* = 0 m). The control parameters of the ASMPC algorithm were determined according to Table 1. Based on the above conditions, the path tracking system of the vehicle was tested at working speeds of 1.0, 2.0, and 3.5 m/s. The reference path and test results are shown in Figures 9–11, respectively. The statistical data of the test results are shown in Table 7.

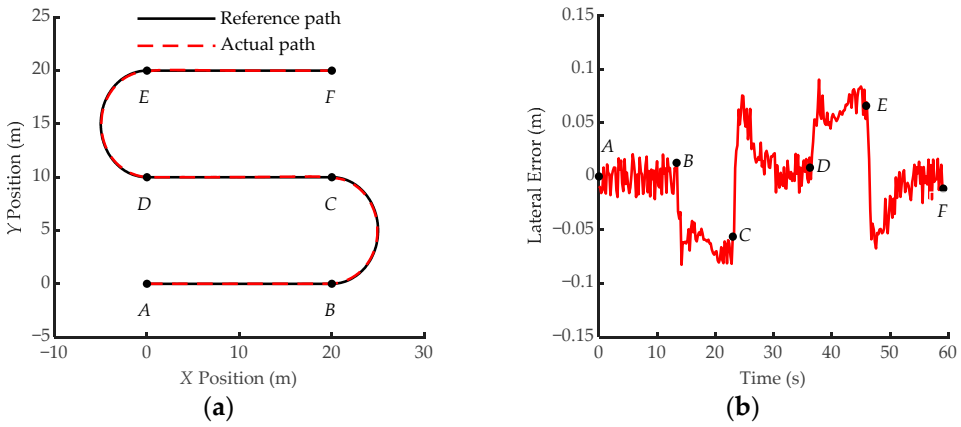


Figure 9. Field test results of path tracking for ASMPC algorithm at the working speed of 1.0 m/s. (**a**) Tracking trajectory; (**b**) Tracking error.

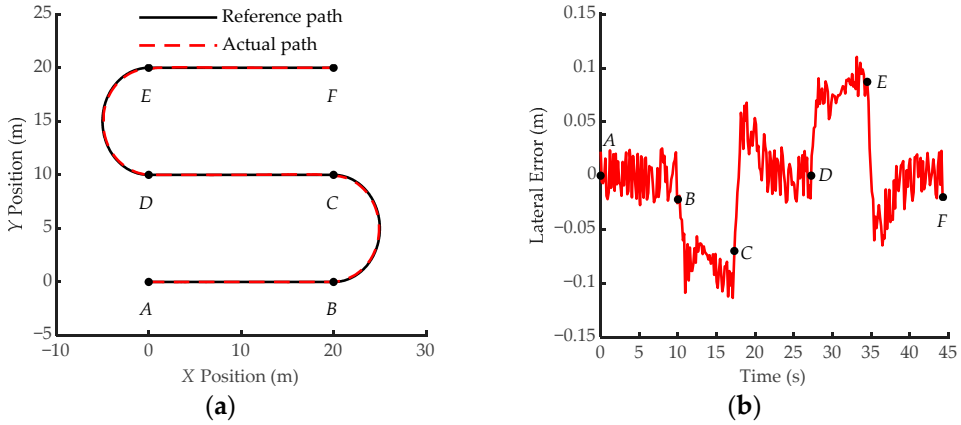


Figure 10. Field test results of path tracking for ASMPC algorithm at the working speed of 2.0 m/s. (**a**) Tracking trajectory; (**b**) Tracking error.

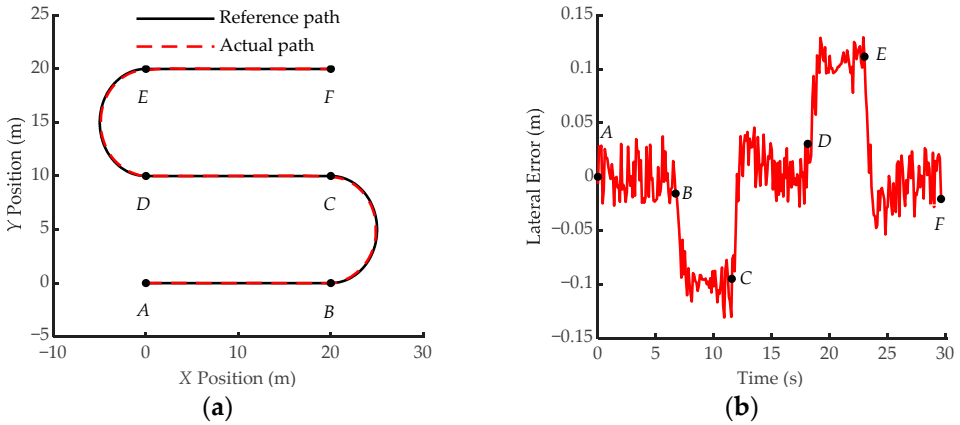


Figure 11. Field test results of path tracking for ASMPC algorithm at the working speed of 3.5 m/s. (**a**) Tracking trajectory; (**b**) Tracking error.

Table 7. Statistical data of field test results for ASMPC algorithm.

Working Speed (m/s)	Maximum Absolute Value of Lateral Error (cm)	RMS Value of Lateral Error (cm)		
	Whole Path	Whole Path	Straight Path	Curve Path
1.0	9.1	3.2	1.7	5.3
2.0	11.3	4.1	1.8	6.5
3.5	13.2	5.8	2.1	8.7

As shown in Figures 9–11, the ASMPC algorithm could control the vehicle to track the reference path stably under different working speeds, but the lateral error curve had local fluctuations which increased slightly with the increase of the working speed, and the maximum absolute value of the lateral error occurred near the junction of the straight path and curve path. When the working speed was 1.0 m/s, the maximum absolute value and RMS value of the lateral error for the whole path were 9.1 and 3.2 cm, respectively, and the RMS values of the lateral error for the straight path and curve path were 1.7 and 5.3 cm, respectively. When the working speed was 2.0 m/s, the maximum absolute value and RMS value of the lateral error for the whole path were 11.3 and 4.1 cm, respectively, and the RMS values of the lateral error for the straight path and curve path were 1.8 and 6.5 cm, respectively. When the working speed was 3.5 m/s, the maximum absolute value and RMS value of the lateral error for the whole path were 13.2 and 5.8 cm, respectively, and the RMS values of the lateral error for the straight path and curve path were 2.1 and 8.7 cm, respectively. At the same working speed, the RMS value of the lateral error increased less with the increase of the reference path curvature, which indicated that the path tracking system had strong robustness to the change of the reference path curvature in terms of control precision. For the same reference path, the maximum absolute value and RMS value of the lateral error increased less with the increase of the working speed, which showed that the path tracking system had strong robustness to the change of the working speed in terms of control precision.

In summary, within the speed range of 1.0 to 3.5 m/s, suitable for field working, the RMS values of the lateral error for the straight path and curve path were no more than 2.1 and 8.7 cm, respectively; hence, the control precision and robustness of the proposed ASMPC algorithm could meet the requirements of field work for wheeled agricultural vehicles.

5. Conclusions

In this paper, an ASMPC algorithm was designed by combining the SMC algorithm with the MPC algorithm and using the fuzzy logic methodology to adjust the prediction horizon and the control horizon. Compared with the third conventional SMPC algorithm, the proposed ASMPC algorithm has two improvements, i.e., removing the sliding mode approach law and incorporating the fuzzy logic methodology, thus effectively improving the control precision and robustness of the path tracking system for wheeled agricultural vehicles.

The simulation results using CarSim and MATLAB/Simulink were as follows: For the straight path tracking at different working speeds, the lateral error of the ASMPC algorithm without the chattering phenomenon asymptotically approached 0 cm, and the dynamic performance and control precision of the ASMPC algorithm were better than those of the conventional MPC algorithm and traditional SMC algorithm. When the working speeds were 1, 3, and 5 m/s, the overshoot of the straight path tracking was 0.34%, 0.09%, and 0.60%, respectively, and the on-line time of the straight path tracking was 3.7, 2.6, and 2.4 s, respectively. For the curve path tracking under different path curvatures, the control precision of the ASMPC algorithm was better than that of the conventional MPC algorithm. When the curvature radiuses of the reference path were 20, 15, and 10 m, the maximum absolute values of the lateral error at a working speed of 3 m/s were 6.9, 8.4, and 10.9 cm, respectively, and the RMS values of the lateral error at a working speed of 3 m/s were 2.8, 3.9 and 6.1 cm, respectively. Moreover, compared with the conventional MPC algorithm and traditional SMC algorithm, the ASMPC algorithm displayed greater robustness to the changes of the working speed and path curvature in terms of control precision.

The field test results show that within a working speed range of 1.0 to 3.5 m/s, the ASMPC algorithm can control a vehicle to track the reference path stably and quickly, and the RMS values of the lateral error for the straight path and curve path do not exceed 2.1 and 8.7 cm, respectively. The proposed ASMPC algorithm can meet the actual working requirements of wheeled agricultural vehicles. This paper introduces the SMPC algorithm into the field of automatic driving for agricultural vehicles and can serve as a reference for SMPC research on the path tracking of wheeled agricultural vehicles. Because the control parameters of the proposed ASMPC algorithm are coupled in the matrices of the control law, it is very difficult to theoretically prove the closed-loop system stability; this will be a follow-up research direction.

Author Contributions: Conceptualization, W.L. and J.Z.; methodology, W.L. and R.G.; software, W.L.; validation, W.L. and R.G.; formal analysis, W.L. and J.Z.; investigation, R.G.; resources, J.Z.; data curation, W.L.; writing—original draft preparation, W.L.; writing—review and editing, W.L.; visualization, W.L. and R.G.; supervision, R.G. and J.Z.; project administration, J.Z.; funding acquisition, R.G. All authors have read and agreed to the published version of the manuscript.

Funding: This research was funded by the National Natural Science Foundation of China (52075469 and 12173054).

Data Availability Statement: The data supporting the findings of this study are contained within the article.

Conflicts of Interest: Author Jingyi Zhao was employed by the Limited Company of Yanda-Yihua Electromechanical Engineering Technology Research Institute, Qinhuangdao, China. The remaining authors declare that the research was conducted in the absence of any commercial or financial relationships that could be construed as a potential conflict of interest.

References

1. Lan, Y.; Zhao, D.; Zhang, Y.; Zhu, J. Exploration and development prospect of eco-unmanned farm modes. *Trans. Chin. Soc. Agric. Eng.* **2021**, *37*, 312–327.
2. Liu, C.; Lin, H.; Li, Y.; Gong, L.; Miao, Z. Analysis on status and development trend of intelligent control technology for agricultural equipment. *Trans. Chin. Soc. Agric. Mach.* **2020**, *51*, 1–18.
3. Li, S.; Xu, H.; Ji, Y.; Cao, R.; Zhang, M.; Li, H. Development of a following agricultural machinery automatic navigation system. *Comput. Electron. Agric.* **2019**, *158*, 335–344. [CrossRef]
4. Li, S.; Zhang, M.; Ji, Y.; Zhang, Z.; Cao, R.; Chen, B.; Li, H.; Yin, Y. Agricultural machinery GNSS/IMU-integrated navigation based on fuzzy adaptive finite impulse response Kalman filtering algorithm. *Comput. Electron. Agric.* **2021**, *191*, 106524. [CrossRef]
5. Yin, X.; Wang, Y.; Chen, Y.; Jin, C.; Du, J. Development of autonomous navigation controller for agricultural vehicles. *Int. J. Agric. Biol. Eng.* **2020**, *13*, 70–76. [CrossRef]
6. Xu, G.; Chen, M.; He, X.; Pang, H.; Miao, H.; Cui, P.; Wang, W.; Diao, P. Path following control of tractor with an electro-hydraulic coupling steering system: Layered multi-loop robust control architecture. *Biosyst. Eng.* **2021**, *209*, 282–299. [CrossRef]
7. Wang, L.; Liu, F.; Song, Z.; Ni, Y.; He, Z.; Zhai, Z.; Zhu, Z.; Zhou, Q.; Song, Z.; Li, Z. Advances in tractor rollover and stability control: Implications for off-road driving safety. *Comput. Electron. Agric.* **2024**, *226*, 109483. [CrossRef]
8. Ding, C.; Ding, S.; Wei, X.; Mei, K. Composite SOSM controller for path tracking control of agricultural tractors subject to wheel slip. *ISA Trans.* **2022**, *130*, 389–398. [CrossRef] [PubMed]
9. Wang, H.; Wang, G.; Luo, X.; Zhang, Z.; Gao, Y.; He, J.; Yue, B. Path tracking control method of agricultural machine navigation based on aiming pursuit model. *Trans. Chin. Soc. Agric. Eng.* **2019**, *35*, 11–19.
10. Zhang, C.; Dong, W.; Xiong, Z.; Hu, Z.; Wang, D.; Ding, Y. Design and experiment of fuzzy adaptive pure pursuit control of crawler-type rape seeder. *Trans. Chin. Soc. Agric. Mach.* **2021**, *52*, 105–114.
11. Yang, Y.; Li, Y.; Wen, X.; Zhang, G.; Ma, Q.; Cheng, S.; Qi, J.; Xu, L.; Chen, L. An optimal goal point determination algorithm for automatic navigation of agricultural machinery: Improving the tracking accuracy of the pure pursuit algorithm. *Comput. Electron. Agric.* **2022**, *194*, 106760. [CrossRef]
12. Zhang, C.; Gao, G.; Zhao, C.; Li, L.; Li, C.; Chen, X. Research on 4WS agricultural machine path tracking algorithm based on fuzzy control pure tracking model. *Machines* **2022**, *10*, 597. [CrossRef]
13. Cui, B.; Sun, Y.; Ji, F.; Wei, X.; Zhu, Y.; Zhang, S. Study on whole field path tracking of agricultural machinery based on fuzzy Stanley model. *Trans. Chin. Soc. Agric. Mach.* **2022**, *53*, 43–48, 88.
14. Sun, Y.; Cui, B.; Ji, F.; Wei, X.; Zhu, Y. The full-field path tracking of agricultural machinery based on PSO-Enhanced fuzzy Stanley model. *Appl. Sci.* **2022**, *12*, 7683. [CrossRef]
15. Ding, Y.; Xia, Z.; Peng, J.; Hu, Z. Design and experiment of the single-neuron PID navigation controller for a combine harvester. *Trans. Chin. Soc. Agric. Eng.* **2020**, *36*, 34–42.
16. Wang, S.; Yin, C.; Gao, J.; Sun, Q. Lateral displacement control for agricultural tractor based on cascade control structure. *Int. J. Control Autom. Syst.* **2020**, *18*, 2375–2385. [CrossRef]
17. Zhang, S.; Wei, X.; Liu, C.; Ge, J.; Cui, X.; Wang, F.; Wang, A.; Chen, W. Adaptive path tracking and control system for unmanned crawler harvesters in paddy fields. *Comput. Electron. Agric.* **2025**, *230*, 109878. [CrossRef]
18. Fan, X.; Wang, J.; Wang, H.; Yang, L.; Xia, C. LQR trajectory tracking control of unmanned wheeled tractor based on improved quantum genetic algorithm. *Machines* **2023**, *11*, 62. [CrossRef]
19. Ahn, D.-V.; Kim, K.; Oh, J.; Seo, J.; Lee, J.W.; Park, Y.-J. Optimal control of semi-active suspension for agricultural tractors using linear quadratic gaussian control. *Sensors* **2023**, *23*, 6474. [CrossRef]
20. Zhang, T.; Jiao, X.; Lin, Z. Finite time trajectory tracking control of autonomous agricultural tractor integrated nonsingular fast terminal sliding mode and disturbance observer. *Biosyst. Eng.* **2022**, *219*, 153–164. [CrossRef]
21. Matveev, A.S.; Hoy, M.; Katupitiya, J.; Savkin, A.V. Nonlinear sliding mode control of an unmanned agricultural tractor in the presence of sliding and control saturation. *Robot. Auton. Syst.* **2013**, *61*, 973–987. [CrossRef]
22. Ge, Z.; Man, Z.; Wang, Z.; Bai, X.; Wang, X.; Xiong, F.; Li, D. Robust adaptive sliding mode control for path tracking of unmanned agricultural vehicles. *Comput. Electr. Eng.* **2023**, *108*, 108693. [CrossRef]
23. Ji, X.; Ding, S.; Wei, X.; Cui, B. Path tracking of unmanned agricultural tractors based on a novel adaptive second-order sliding mode control. *J. Frankl. Inst.* **2023**, *360*, 5811–5831. [CrossRef]
24. Ding, S.; Huang, C.; Ding, C.; Wei, X. Straight-line tracking controller design of agricultural tractors based on third-order sliding mode. *Comput. Electr. Eng.* **2023**, *106*, 108559. [CrossRef]
25. Sun, J.; Wang, Z.; Ding, S.; Xia, J.; Xing, G. Adaptive disturbance observer-based fixed time nonsingular terminal sliding mode control for path-tracking of unmanned agricultural tractors. *Biosyst. Eng.* **2024**, *246*, 96–109. [CrossRef]
26. Huang, W.; Wei, X.; Wang, A.; Ji, X.; Gao, Y.; Wang, Y.; Shi, S. Straight line path tracking control of agricultural tractor-trailer based on fuzzy fast sliding mode. *Trans. Chin. Soc. Agric. Mach.* **2024**, *55*, 415–422.

27. Ding, Y.; Wang, L.; Li, Y.; Li, D. Model predictive control and its application in agriculture: A review. *Comput. Electron. Agric.* **2018**, *151*, 104–117. [CrossRef]
28. Chi, R.; Xiong, Z.; Jiang, L.; Ma, Y.; Huang, X.; Zhu, X. Path tracking control algorithm of transplanter based on model prediction. *Trans. Chin. Soc. Agric. Mach.* **2022**, *53*, 22–30, 99.
29. Liu, Z.; Zhang, W.; Lü, Z.; Zheng, W.; Mu, G. Design and test of path tracking controller based on nonlinear model prediction. *Trans. Chin. Soc. Agric. Mach.* **2018**, *49*, 23–30.
30. Lu, G.; Xu, J. Research on path tracking of tractors based on adaptive model predictive control. *J. Shandong Univ. Nat. Sci.* **2022**, *36*, 24–29.
31. Cheng, S.; Li, L.; Chen, X.; Wu, J.; Wang, H. Model-predictive-control-based path tracking controller of autonomous vehicle considering parametric uncertainties and velocity-varying. *IEEE Trans. Ind. Electron.* **2021**, *68*, 8698–8707. [CrossRef]
32. Park, G.; Choi, S.B. A model predictive control for path tracking of electronic-four-wheel drive vehicles. *IEEE Trans. Veh. Technol.* **2021**, *70*, 11352–11364. [CrossRef]
33. Zhang, Y.; Edwards, C.; Belmont, M.; Li, G. Robust model predictive control for constrained linear system based on a sliding mode disturbance observer. *Automatica* **2023**, *154*, 111101. [CrossRef]
34. He, L.; Xu, Z.; Huang, C.; Gong, C.; Li, S.; Shi, Q. Research on sliding mode control algorithm for angle tracking prediction of steer-by-wire system. *Automot. Eng.* **2023**, *45*, 2200–2208.
35. Liu, Q.; Zhang, L.; Xiao, Y.; Zhang, L.; Fan, G. Predictive sliding mode control for flexible spacecraft attitude tracking with multiple disturbances. *Control Eng. Pract.* **2025**, *154*, 106160. [CrossRef]
36. Liu, C.; Liu, H.; Han, L.; Nie, S. Learning-based sliding mode predictive trajectory tracking and stability control for autonomous vehicle in unstructured environments. *J. Mech. Eng.* **2024**, *60*, 399–412.
37. Duan, X.; Tao, J.; Qin, C.; Cai, D.; Li, Y.; Liu, C. Agricultural machinery path tracking stability control method under variable speed conditions. *Trans. Chin. Soc. Agric. Mach.* **2019**, *50*, 18–24, 32.
38. Yue, X.; Chen, J.; Li, Y.; Zou, R.; Sun, Z.; Cao, X.; Zhang, S. Path tracking control of skid-steered mobile robot on the slope based on fuzzy system and model predictive control. *Int. J. Control Autom. Syst.* **2022**, *20*, 1365–1376. [CrossRef]
39. Yao, Y.; Chen, X.; Ji, C.; Chen, J.; Zhang, H.; Pan, F. Design and experiments of the single driver for maize precision seeders based on fuzzy PID control. *Trans. Chin. Soc. Agric. Eng.* **2022**, *38*, 12–21.
40. Chen, H.-C.; Xu, S.-Y.; Deng, K.-H. Water color identification system for monitoring aquaculture farms. *Sensors* **2022**, *22*, 7131. [CrossRef]
41. Zhu, D.; Gao, Q. Sliding mode variable structure control of PMSM based on improved exponential reaching law. *Agric. Equip. Veh. Eng.* **2023**, *61*, 111–116.

Disclaimer/Publisher's Note: The statements, opinions and data contained in all publications are solely those of the individual author(s) and contributor(s) and not of MDPI and/or the editor(s). MDPI and/or the editor(s) disclaim responsibility for any injury to people or property resulting from any ideas, methods, instructions or products referred to in the content.